



Naif Arab University for Security Sciences
Arab Journal of Forensic Sciences & Forensic Medicine

المجلة العربية لعلوم الأدلة الجنائية والطب الشرعي
<https://journals.nauss.edu.sa/index.php/AJFSFM>



ATR FT-IR Spectroscopy: A Novel and Non-Destructive Approach for the Detection of Blood on a Single Fiber



التحليل الطيفي ATR FT-IR: مقارنة جديدة وغير متلفة لعينة للكشف عن الدم الموجود على فتيلة خيط واحدة

Sweety Sharma¹, Jaskirandeep K. Jossan¹, Rajinder Singh^{2*}

¹ Senior research fellow, Department of forensic science, Punjabi University, Patiala, India.

^{2*} Associate Professor, Department of Forensic Science, Punjabi University, Patiala, India.

Received 04 Jan. 2020; Accepted 08 Apr. 2020; Online 15 Jun. 2020.

Abstract

Blood is often encountered on different types of substrates in criminal investigations. Among such substrates, blood stained fabrics are one of the most commonly encountered evidence. Analysis of bloodstains on fabrics is restricted due to interference of fabric dyes, color of fabric which hampers visual identification, and limited sample quantity. Over the years, a plethora of research has been conducted to analyze recovered blood traces, however, the methods employed are limited by factors such as sample destructibility, chronophagus processing, and vulnerability to false positive results. To circumvent the aforementioned limitations, use of ATR FT-IR spectroscopy has surged as a non-destructive and reliable tool for the detection of traces of blood and other body fluids on fibers. In the present study, an attempt has been made to detect traces of blood in fibers of different types and colors using ATR FT-IR spectroscopy. The obtained results unequivocally concluded that by using ATR FT-IR spectroscopy blood can be successfully detected even on a single fiber through characteristic peaks positioned at 1650 cm⁻¹ and 1543 cm⁻¹ corresponding to amide I and amide II. On the basis of the IR marked protein region

المستخلص

غالبًا ما يتصادف وجود الدم على أنواع مختلفة من الركائز (العينات) في التحقيقات الجنائية. ومن بين هذه الركائز، تعتبر الأقمشة الملطخة بالدم واحدة من الأدلة الأكثر شيوعًا. تحليل بقع الدم على الأقمشة مقيد بسبب تداخل أصباغ النسيج ولون النسيج الذي يعيق التحديد البصري وكمية العينة المحدودة. على مر السنين، تم إجراء عدد كبير من الأبحاث لتحليل آثار الدم المرفوعة من الأدلة (العينات) المختلفة، ومع ذلك، فإن الأساليب المستخدمة محدودة بعوامل مثل تدمير العينة، وطول فترة المعالجة، والتعرض لنتائج إيجابية خاطئة. للتغلب على القيود المذكورة أعلاه، ازداد استخدام التحليل الطيفي ATR FT-IR كأداة غير متلفة وموثوقة للكشف عن آثار الدم وسوائل الجسم الأخرى على فتلات الخيوط. في هذه الدراسة، جرت محاولة للكشف عن آثار الدم في الألياف من مختلف الأنواع والألوان باستخدام التحليل الطيفي ATR FT-IR.

النتائج التي تم الحصول عليها خلصت بشكل لا لبس فيه إلى أنه باستخدام التحليل الطيفي ATR FT-IR، يمكن الكشف عن الدم بنجاح حتى على ألياف خيوط مفردة من خلال القمم المميزة الموضوعية عند 1650 و 1543 سم⁻¹، المقابلة للأياميد الأول والأياميد الثاني، على أساس منطقة البروتين التي تحمل علامة الأشعة تحت

Keywords: Forensic Science, Forensic Serology, Fibers, Fourier Transform Infrared Spectroscopy

الكلمات المفتاحية: علوم الأدلة الجنائية، أمصال الأدلة الجنائية، الكشف، الألياف، التحليل الطيفي بالأشعة تحت الحمراء



Production and hosting by NAUSS



* Corresponding Author: Rajinder Singh

Email: rajchandel7@gmail.com

doi: [10.26735/AYFK5009](https://doi.org/10.26735/AYFK5009)

(1700-1500 cm^{-1}) bloodstains could easily be discriminated from the blank fibers (except human hair, which overlapped with the peaks of bloodstained fibers) by using PCA chemometric tool. Although, further investigations are needed to be conducted, this proof-of-concept study establishes the potential use of ATR FT-IR spectroscopy for the non-destructive, rapid, eco-friendly, and reliable identification of blood traces from a single fiber due to its inherent surface sensitivity and smaller penetration depth.

الحمراء (١٧٠٠-١٥٠٠ سم^{-١}) يمكن تمييز بقع الدم بسهولة من الألياف الفارغة (باستثناء الشعر البشري، الذي يتداخل مع قمم الألياف الملطخة بالدم) باستخدام الأداة الكيمومترية PCA. وعلى الرغم من الحاجة إلى إجراء مزيد من الفحوص، فإن دراسة إثبات المفهوم هذه، حددت الاستخدام المحتمل لمطياف ATR FT-IR من أجل التعرف على آثار الدم كأداة غير متلفة وسريعة وصديقة للبيئة والموثوقة من ألياف خيوط واحدة بسبب حساسية السطح المتضمن وصغر عمق الاختراق.

1. Introduction

Out of all body fluids inevitably encountered at a crime scene, blood is the most significant and frequently studied body fluid. However, its analysis on stained fiber is still a fairly unexplored niche. There are certain limitations associated with the detection of blood on fabrics. Firstly, fibers may interfere and contaminate blood samples and their subsequent extraction and identification can be difficult to comprehend and time consuming, if not impossible. Secondly, the color of the fabric can obstruct the visual detection of blood. Thirdly, sometimes the actual number of fibers containing trace amount of blood are limited which makes it even harder to detect blood due to lack of sufficient quantity. There is an essential need for more research analysis and to utilize techniques which can detect the presence of blood and at the same time eliminate interference caused due to the colors and substrates [1-3].

Through many decades of research studies, several presumptive and confirmatory tests have been made available to check whether a particular stain is or not blood. The presumptive tests are most commonly based on the oxidation reduction mechanisms, which are destructive in nature and, therefore, identification of blood using these tests comes at a cost of sample destruction [1,4,5]. Another limitation of these presumptive tests is that they are non-specific, time-consuming, expensive, ambiguous, hazardous to both humans and environment, and dependent on the expert's judgment. These limitations could be avoided by using non-destructive tools with greater versatility and objectivity that not only maintains the integrity of sample but are more informative, sensitive, and reliable [1].

In the last decade, various biological approaches based on micro RNA (miRNA) [6-11], messenger RNA (mRNA) [3,12-14], Piwi-interacting RNA (piRNA) [15], CircRNA (circular RNA) [16], and DNA methylation [17-26] have been established for the confirmatory

identification of blood. While these methods provide confirmatory results, these methodologies are expensive, time-consuming, require extensive laboratory conditions, and therefore are not ideal for the routine analysis of blood.

Therefore, other techniques such as spectroscopic methods have been explored for the identification and discrimination of body fluids due to their sensitive, rapid, non-destructive nature and at the same time its applicability for multiple body fluid analysis. Ultraviolet visible (UV-Vis) spectroscopy was the first spectroscopic technique evolved with the localization of blood and other body fluid stains. However, false positive results and lack of selectivity have limited its utility in identifying body fluid stains on colored substrates [27-30].

Further, vibrational spectroscopy including Raman spectroscopy and Attenuated Total Reflectance (ATR) Fourier Transform Infrared spectroscopy (FT-IR) spectroscopy have emerged as well suited techniques for body fluid analysis [31]. Lednev's team have pioneered the use of Raman spectroscopy for the analysis of various body fluids and other researchers have extended this study [32-39]. Besides identification of body fluids, origin of blood (animal or human origin), [40-43], race differentiation [44,45], sex determination [46] and even discrimination between same type of body fluid such as peripheral blood and menstrual blood [47] has been successfully achieved. Even though, Raman spectroscopy provides satisfactory results for the identification and discrimination of blood and other body fluids, the intense Raman signals generated from stained fabrics due to the presence of dye components cause obstruction in the identification on the stained fabric substrates [38,48]. Moreover, the cost of Raman spectroscopy is very high when compared with ATR FT-IR spectroscopy [49]. In contrast, FTIR spectroscopy has been shown to provide promising results and has been described as a great



potential tool to detect blood stains on fabric substrates due to its inherent surface sensitivity and less penetration depth [30,49,50]. This technique is rapid, confirmatory (qualitative and quantitative), sensitive, non-destructive, environment friendly, no consumables-cost, and little-to-no sample preparation is required during analysis [2,31,51]. The major advantage of this instrument is that it is readily available in forensic laboratories and its hand-held devices are also available to facilitate on the spot identification.

In recent years, ATR FT-IR spectroscopy has garnered wide attention for the forensic identification and discrimination of various types of body fluids [2,49–54]. This technique has also been used for age estimation, human vs animal body fluids (species identification) [55–57], and to discriminate between post-mortem and ante-mortem blood on various substrates [58,59]. Another progress has been made on phenotype profiling for the determination of sex of an individual [60], and also effects on the causes of death on postmortem interval estimation were also evaluated using the same technique [61].

ATR FT-IR spectroscopy has been used to identify blood signature absorbance bands in the mid infrared range of 4000-6000 cm^{-1} attributed to Amide A ($\sim 3300 \text{ cm}^{-1}$); Amide B ($2800\text{-}3000 \text{ cm}^{-1}$); Amide I ($\sim 1650 \text{ cm}^{-1}$); Amide II ($\sim 1540 \text{ cm}^{-1}$); and Amide III ($\sim 1200\text{-}1350 \text{ cm}^{-1}$) [2,49,62,63]. Furthermore, ATR FT-IR spectroscopy offers a penetration depth of less than $10 \mu\text{m}$ which enables detection of blood traces on highly absorbing surfaces such as cloth fabric [62]. Results obtained with this technique are in the form of bands or peaks, representative of the functional groups and the position of a peak is specific to particular interactions with molecular bonds that give specific information related to the biochemical composition.

This approach has been extensively used to identify and differentiate various classes of fibers such as cellulosic fibers [64], textile fibers [65], regenerated natural fibers and proteinaceous fibers and many other different types of fibers [66,67]. Hitherto, to the best of author's knowledge no work has been conducted to detect traces of blood on a single fiber using ATR FT-IR spectroscopy.

In the present proof-of concept study, an attempt has been made to identify trace amount of blood from single blood stained fiber. The use of non-destructive ATR FT-IR spectroscopy will allow preservation of samples and facilitate the samples to undergo further DNA typing if required.

2. Materials and Methods

2.1. Sample collection

Blood samples ($n=25$) were collected from twenty-five healthy anonymous donors with due approval from the institutional human ethical committee (IEC/03-2017/08) and were tested as negative for HBsAg (Hepatitis B surface antigen), hepatitis c, and HIV (Human immunodeficiency virus) antigen. Before collecting samples, proper written informed consent was obtained from each volunteer. 2-3 ml of blood was collected in anti-coagulant EDTA (Ethylene di-amine tetra acetic acid) tube.

2.2. Sample preparation

2.2.1 Blood on a glass slide (Neat sample)

To obtain spectrum of neat blood, $50 \mu\text{l}$ of blood was drawn from individual donors by finger prick method using safety lancet (Bio Point Blood Lancet) and deposited on $1 \times 1 \text{ cm}$ marked area of clean glass slide and was allowed to dry for approximately 24 hours at room temperature ($25 \pm 5 \text{ }^\circ\text{C}$). After that sample was scraped out with the help of a sterile spatula, the dried blood was placed directly on the cleaned ATR crystal surface and was scanned three times.

2.2.2 Blood samples on different fibers

Total of 40 fabric samples of 10 different types and human scalp hair (4 each) were collected. Table-1 indicates the details of collected fibers for the deposition of blood. Different set of single fibers were obtained from 3 different types of sources. First type of source include 4 different cotton fabrics (white, blue, red, and black). Second set of source included different fabric compositions including blue denim, jute, blue velvet, knitting yarn, red silk, and polyester. Third set of source includes human scalp hair. A single thread was removed from the fabric substrate with the help of fine-pointed tweezers. Five cm portion of thread (lengthwise) was cut and $10 \mu\text{l}$ of blood was deposited on these threads and were allowed to dry at room temperature for 2-4 hours for further analysis. In addition, four samples of un-dyed human hair were collected from four donors using simple combing method.

2.3 Blood look-alike substances

Three samples each of 10 similar looking non-blood substances including cosmetics and other products of daily use such as red lipstick, red eye-shadow, red nail polish, red ink, vermilion, honey, procure liquid hand wash (strawberry), red fiber, red dye, and red skin toner



Table 1- Details of collected fibers for the deposition of blood.

S.No.	Source of Fibers	Number of samples
1	White cotton	04
2	Blue cotton	04
3	Red cotton	04
4	Black cotton	04
5	Blue denim	04
6	Knitting yarn	04
7	Nylon	04
8	Jute	04
9	Blue velvet	04
10	Polyester	04
11	Human scalp hair	04

were collected and directly smeared on glass slide and then allowed to dry for 24-hrs at ambient conditions. After drying, blood samples were scraped out using sterile spatula and approximately 15-20 mg samples of dried smears were taken for analysis.

2.4 Spectral acquisition

The samples were analyzed using Bruker Alpha ATR FT-IR spectrometer accessorized with ZnSe crystal and Deuterated Lanthanum α -Alanine Doped Triglycene Sulphate (DLATGS) detector. To record the spectra OPUS (V 7.2) software was used. Data was saved in

OPUS format. The wave number range selected for the spectra collection was 4000-600 cm^{-1} , that is mid infrared range, and the spectral resolution was set at 4 cm^{-1} with 24 scans. The blank fiber samples were run as a background and the blood stained fibers were analyzed as a sample and then subtraction was done in the whole mid-infrared range. After every analysis the stage was cleaned using a wet ATR cleaning tissue (part No. 1008033), containing deionized water and isopropyl alcohol to remove left-over traces of previous samples to avoid cross contamination.

2.5 Chemometrics

Chemometrics is the application of statistical and mathematical methods to get useful chemical information from very complex data that would otherwise be difficult to interpret [68]. Swedish scientists, Bruce R. Kowalski and Svante Wold were the first to use the term “chemometrics” in 1972.

2.5.1 Unsupervised model- Principal Component analysis (PCA)

PCA is a well known chemometric tool that is used to reduce the data to identify significant variations and similarities between sample groups. It is an exploratory and data reduction tool that creates a new space of orthogonal variables from the linear combination of the original ones. By maximizing the variance in the data set, new variables that are PCs (principal components) are formed, due to which redundant information in the form of noise are eliminated and dimensional reduction can be achieved.

The equation which shows the PCA model structure is [69]:

$$X = TP^t + E$$

Where, X is acquired data matrix; T represents score matrix; P indicate loading matrix; and E shows residual matrix

The aim of PCA is to reduce the large data set into easy comprehensible variables known as principal components and further identifies the natural clusters in the data set using these principal components. First principal component represents the factor explaining the largest possible variation in the data set and second principal component conveying second maximum variation and so forth [68,70].

2.5.2 Pre-processing of data

Pre-processing methods were carried out to reduce the noise in the data set and increase the information



content of a spectrum. It also helps to eliminate the variations in path length. The spectra were pre-processed using baseline offset and linear baseline correction, smoothing by Savitzky-Golay algorithm (2 polynomial order and 11 smoothing points in a symmetric kernel), normalization by range, 7 PCs with SVD (singular value decomposition) algorithm and random cross validation method [70,71].

3. Results and Discussion

The present work was designed to accomplish quick, easy, reliable, and non-destructive detection of blood from a single bloodstained fiber using ATR FT-IR spectroscopy. In this study, blood samples were collected from 25 healthy individual donors and showed no significant intra-donor variation on the basis of their obtained spectra.

3.1 Characterization of blood

Blood is heterogeneous in nature and contains variety of constituents such as fibrinogens, hemoglobin, albumin, RBC, WBC, plasma, platelets, glucose, carbohydrates etc. [51]. ATR FT-IR spectroscopy was used to ascertain the peaks related to proteins and other components of blood. Table-2 shows the ATR FT-IR bands assignments for bloodstains. Reference books and previous research were used to determine the contribution of the proteins and other small molecules present in the spectrum of blood [2,49–51,55–57,72]. Among all the peaks, the one positioned at 1640 cm^{-1} and 1534 cm^{-1} were categorized as the most intense and dominant peaks as rest of the peaks are weak due to their low peak intensity.

3.2 Visual spectral features of fibers

The spectra obtained from cotton fabrics show the major peaks at 1706, 1509, 1465, 1406, 1340, 1241, 1090, 1016, 869, 846, and at 716 cm^{-1} and show a high focus of the cellulose components. The fabrics of blue denim show the important absorbance bands at 1713, 1505, 1408, 1338, 1236, 1084, 1014, 968, 870, 844, and 721 cm^{-1} . Velvet shows the significant peaks at 1645, 1548, 1468, 1427, and at 1369 cm^{-1} , knitted yarn shows major absorbance peaks at 1734, 1448, 1365, 1229, 1067, 1027, and at 764 cm^{-1} . In red silk fiber peaks are observed at 1708, 1463, 1406, 1339, 1239, 1089, 1014, 869, 845, and 710 cm^{-1} , peaks obtained in the jute are positioned at 1736, 1640, 1456, 1424, 1367, 1319, 1236, 1157, 1024, and 663 cm^{-1} , finally in human hair absorbance peaks are positioned at 1632, 1524, 1458, 1404, 1229, 1053, 856, 720, and 674 cm^{-1} .

Table 2- ATR FT-IR bands assignment for bloodstains.

Wavenumbers (cm^{-1})	Band Assignments
~3289	H bonded O-H stretching, and N-H symmetric Stretching (Amide A)
~2955	plasma lipids with CH ₃ stretching vibrational mode
~1640	α - Helical structures of proteins, amide I
~1534	Amide II band
~1446	methyl bending of amino acids, proteins, lipids with asymmetric CH ₃ bending
1456-1395	fibrinogen, haptoglobin, IgA, IgG, and IgM
~1388	fibrinogen and amino acid side groups with symmetric CH ₃ bending
1286-1320	amide III with C-N stretching
1250-925	Carbohydrates (glucose) peaks with C-O symmetric stretching
1150- 950	carbohydrates and sugar moieties

Peak positions at 1711 and 1089 cm^{-1} were assigned to the ester group; with a peak approximately at 1505 cm^{-1} being due to lignin [64]; peak at 1460 cm^{-1} corresponds to C-H- deformation and asymmetric in -CH₃- and -CH₂-; peak positioned at approximately 1425 cm^{-1} is attributed to aromatic skeletal vibration combined with C-H in plane deformation; peak at approximately 1366 cm^{-1} is due to C-H deformation in cellulose and hemicelluloses; peaks at 1338 cm^{-1} due to the -OH in-plane bending [73]. Peak at approximately 1328 cm^{-1} corresponds to syringyl ring plus Guaiacyl ring condensed; Peak at 1236 cm^{-1} corresponds to OH in-plane bending; peak at approximately 1155 cm^{-1} ascribed to C-C ring breathing band or C-O-C vibration in cellulose and hemicelluloses [64,65]. Peak positioned at approximately 1105 cm^{-1}



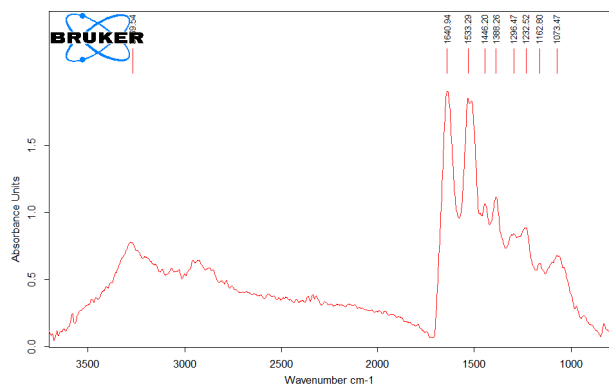


Figure 1- ATR FT-IR spectrum of blood dried overnight at ambient conditions.

Table 3- Vibrational mode associated with Amide peaks.

Amide Peaks	Vibrational Mode
Amide I (Near 1650 cm ⁻¹)	80% C=O stretch
Amide II (Near 1550 cm ⁻¹)	60 % N-H bend and 40% C-N stretch

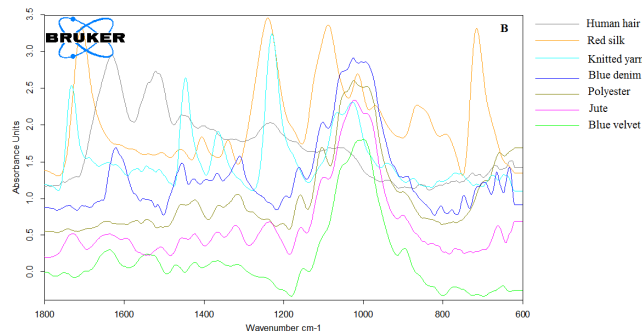
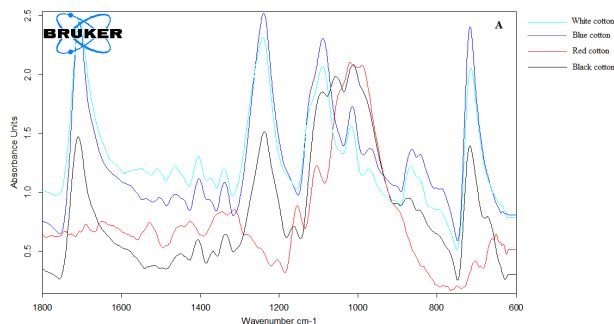


Figure 2- ATR FT-IR spectra of the (A). white and colored cotton fabrics and (B). ATR FT-IR spectra of other fibers including human hair, red silk, knitted yarn, blue denim, polyester, jute, and blue velvet.

is attributed to polysaccharide components (O-H association band in cellulose and hemicelluloses); peak at approximately 1092 and 1014 cm⁻¹ are due to O=C–O–C or secondary alcohol; peak at approximately at 1056 cm⁻¹ corresponds to C–O stretching in cellulose and hemicelluloses; peak at approximately 1031 cm⁻¹ is due to aromatic C–H in plane deformation, guaiacyl type, C–O deformation, and primary alcohol [65]; peak at approximately 971 cm⁻¹ corresponds to C=C vibrational group [74]; peak at approximately 872 cm⁻¹ corresponds to five substituted H in benzene; peak at approximately 869 cm⁻¹ corresponds to five substituted H in benzene; peak at approximately 844 cm⁻¹ attributed to two neighboring H in benzene; peak at 722 cm⁻¹ is attributed to heterocyclic aromatic ring.

3.3 Identifying blood stains on single thread of different fibers

The representative overlaid ATR FT-IR spectra of

neat blood, blood contaminated fibers, and blank fibers have been shown in figure-3 (A-K). The blood peaks can clearly be differentiated in the presence of amide I and amide II positioned approximately at 1640 cm⁻¹ and 1533 cm⁻¹ in bloodstained fibers. Elkins [51], Orphanou [2], and Quinn [49] strongly favor the use of amide I and amide II peaks for the identification of blood, in spite of interference caused by substrates, these two peaks can be very well differentiated. Quinn et al. 2017 [49] suggest that due to interference caused by the substrates the amide I and amide II peak are of low intensity and high noise. In the present study a single fiber thread was used as a substrate, and the high intensity peaks of amide I and amide II were obtained for confirming the presence of blood on the fibers of different types and colors. Findings from different studies suggested that nine characteristics peaks corresponding to different amide groups are significant however amide I and amide II peaks are significant in investigating the secondary structures of proteins [75–78]. Table-3 illustrates the vibrational mode



associated with Amide peaks.

Figure-3(A-K) of the overlaid spectra of blank cotton fibers, neat blood, and bloodstained fibers shows that the spectral signature bands of amide I and amide II were quite different, intense, and sharp. The spectrum of bloodstained fiber was significantly different than the blank cloth fibers in the selected amide range (1700-1500 cm^{-1}). Spectra of blank fiber spectra do not exhibit

peaks in the spectral range of 1700-1500 cm^{-1} that are characteristics of amide I and amide II due to blood proteins. Because of that, it is easier to identify the blood on the selected fiber substrates. This scope of using amide I and amide II peaks to confirm the presence of blood was limited in case of human hair samples as the hair itself contains the protein bands of amide I and amide II in the same region which cannot be differentiated from blood.

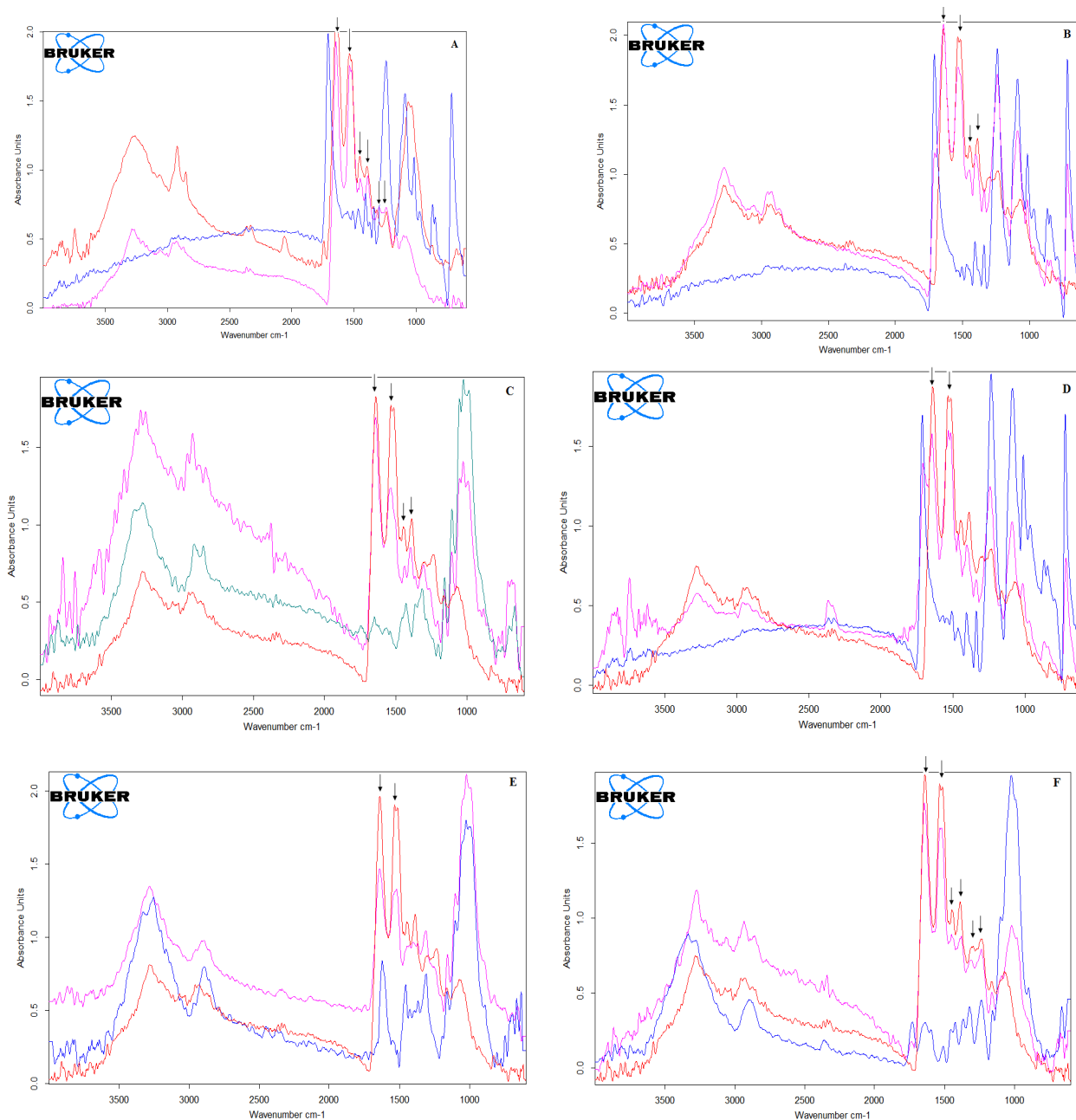
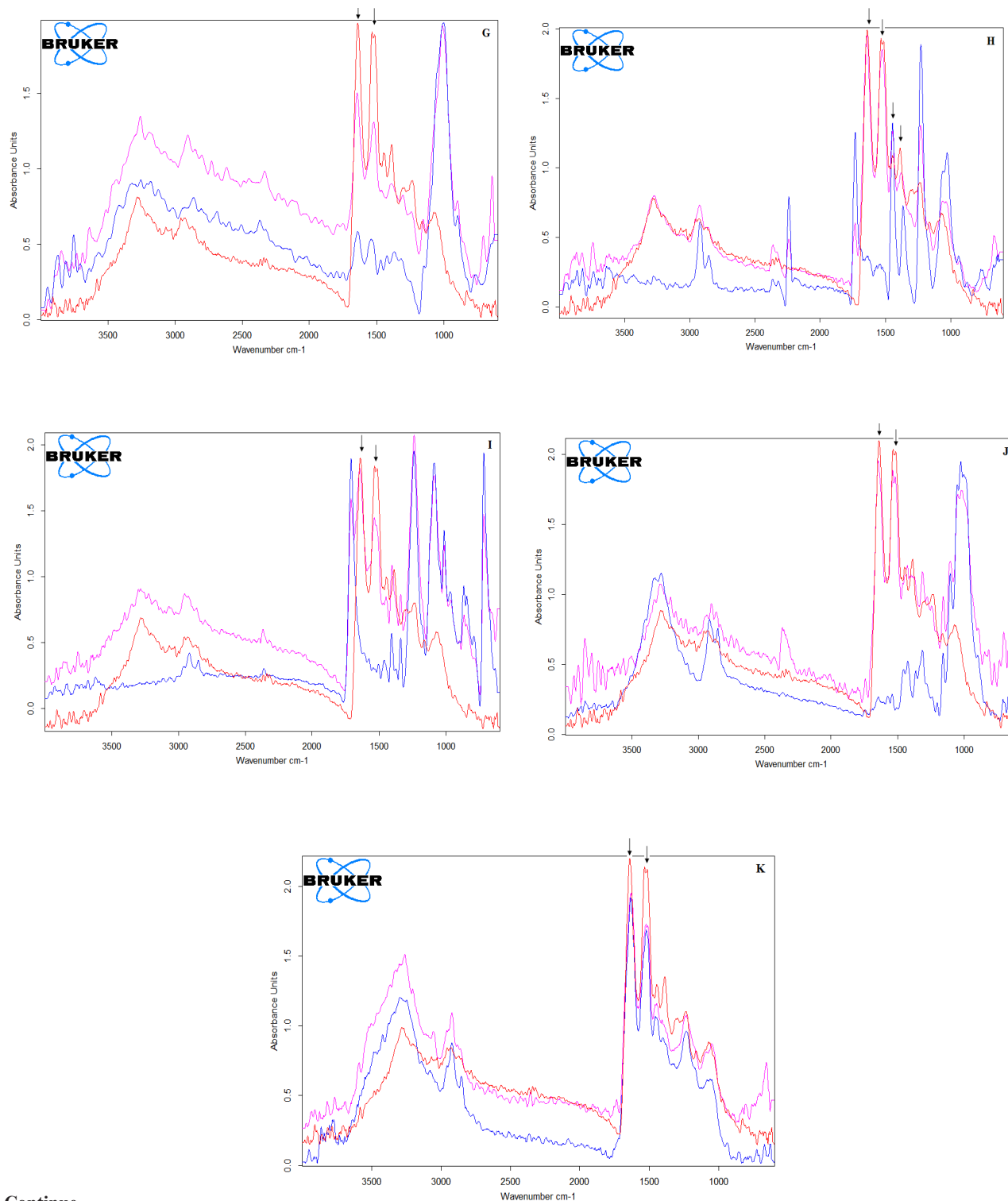


Figure 3- Overlaid ATR FT-IR spectrum of neat blood (red) and neat fiber (blue) and bloodstained fibers (pink) A. White cotton B. blue cotton C. red cotton D. black cotton E. blue denim F. jute G. blue velvet H. knitted yarn I. silk J. Polyester K. Human hair. Bloodstained fibers were dried overnight at ambient conditions.





Continue

Figure 3- Overlaid ATR FT-IR spectrum of neat blood (red) and neat fiber (blue) and bloodstained fibers (pink) A. White cotton B. blue cotton C. red cotton D. black cotton E. blue denim F. jute G. blue velvet H. knitted yarn I. silk J. Polyester K. Human hair. Bloodstained fibers were dried overnight at ambient conditions.



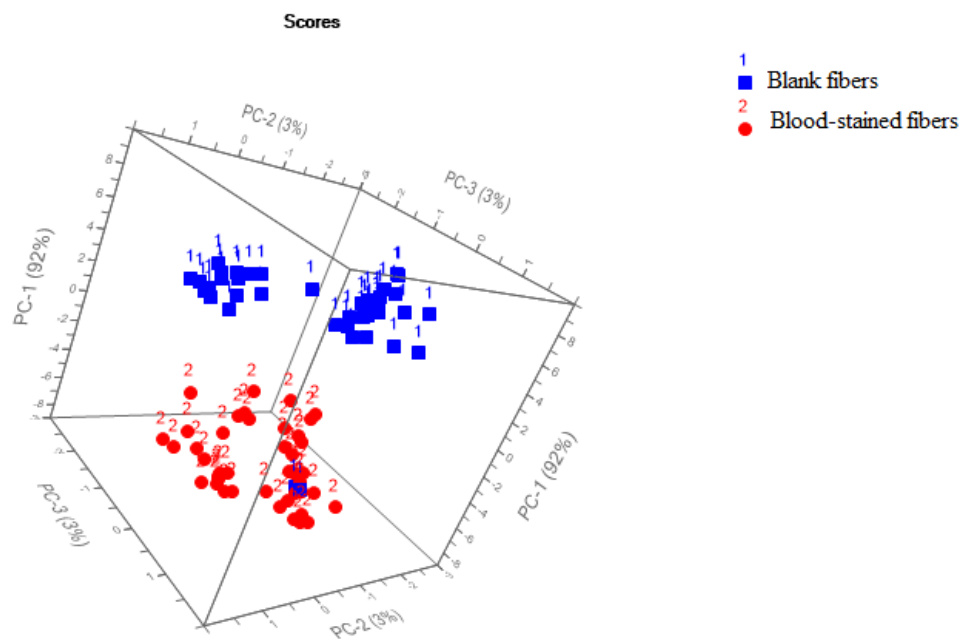


Figure 4a- 3D-PCA score plot to discriminate blood stained fibers from blank fibers (1700-1500 cm^{-1})

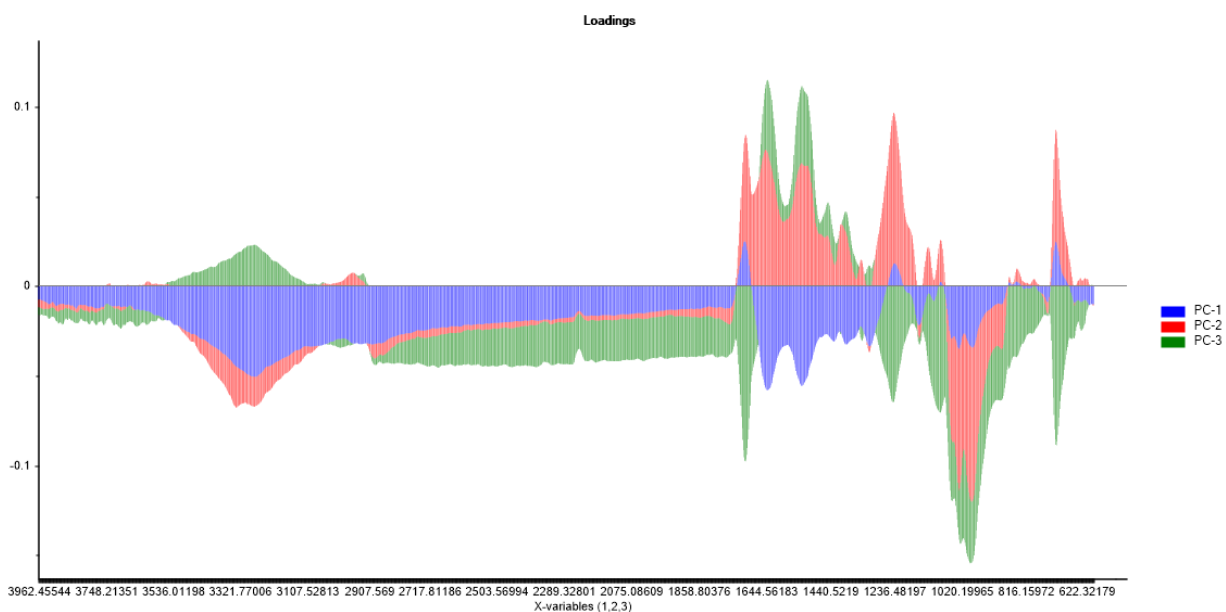


Figure 4b- Correlation line loading plot of PC1, PC2, and PC3.



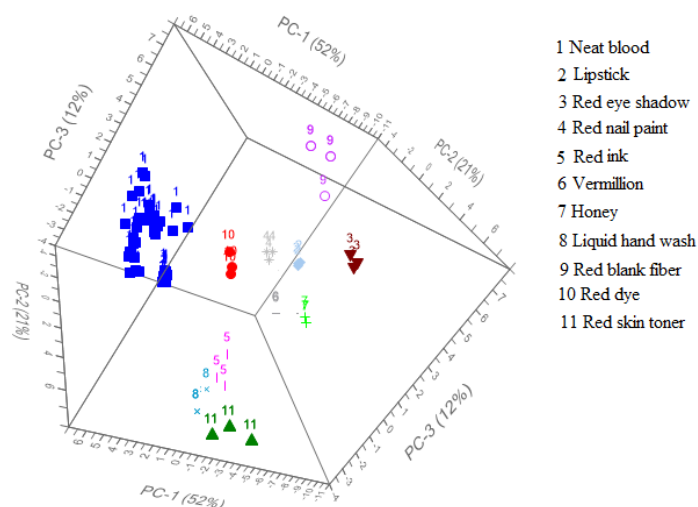


Figure 5a- Three dimensional PCA-score plot of the spectra from the neat blood and non-blood substances.

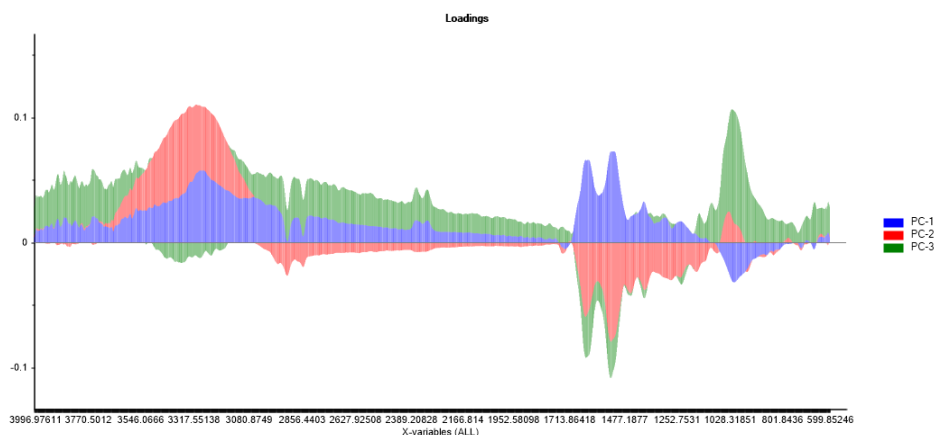


Figure 5b- Combined line loadings plot from PC1 (blue), PC2 (red), and PC3 (green) to discriminate blood from non-blood substances.

Therefore, it would be a difficult task to identify blood traces on human hair fiber due to its overlapping peaks of amides in the same region (Figure-3k).

The dye present in the fabric substrates goes undetectable by FTIR spectroscopy and therefore does not cause any interference in the identification of bloodstains. This study in particular is interesting, in view of the fact that it has already been described that the fabric color presents numerous limitations by UV-Vis spectroscopy but it can be overcome by ATR FT-IR spectroscopy [30]. The results of the present work concluded that the type and color of the fibers had no significant effect on the detection of bloodstains on fiber substrates. Therefore, ATR FT-IR spectroscopy is suitable to detect blood stains on single fibers.

Figure-4a shows the results of PCA differentiating

bloodstained fibers from blank fiber spectra using the most discriminating wave number range of amide I and amide II ($1700-1500\text{ cm}^{-1}$). Results of PCA showed a clear separation between blank fibers (class-1) and bloodstained fibers (class-2) in the selected range. Only blank human hair fibers were misclassified in class 2 of bloodstained fibers. The PCA model proved that the amide I and amide II region can be considered as the spectral region with least substrate interference and this statement was also supported by the previous literature [2,30,50,53]. According to the PCA results, the spectral range of $1700-1500\text{ cm}^{-1}$ was considered as optimum for the discrimination of bloodstained fibers and neat fibers as this range presented no interference due to the peaks obtained from the spectra of blank fibers. The cumulative variance of PC1, PC2, and PC3 summarized 98% of



the PCA model. Specifically, PC1 explains 92 % of the initial variation, PC2 accounted for next 3% of variation, and PC3 accounted for remaining 3% of variation in the data set (Figure-4a). First three principal components (PC1, PC2, and PC3) are sufficient to discriminate the pre-established classes of blank fibers and blood contaminated fibers. The spectra of bloodstained fibers were distributed along with the negative values of PC1 and spectra of blank fibers were distributed towards the positive values of PC1. Figure-4b shows the combined loading plot of PC1, PC2, and PC3. The loadings plot exhibits the similar profile as the original data and it highlights the regions of high importance which convey significant information. The PCA loading plot can be divided into 8 regions. Region 1 (4000-3554 cm^{-1}), where PC1, PC2, and PC3 show negative correlation; Region 2 (3554- 3054 cm^{-1}), where PC1 and PC2 show negative correlation and PC3 shows positive correlation; Region 3 (2913-1740 cm^{-1}), where PC1, PC2, and PC3 all show negative correlation; Region 4 (1740-1693 cm^{-1}), where PC1 and PC2 show positive correlation and PC3 shows negative correlation; Region 5 (1687-1320 cm^{-1}), where PC2 and PC3 show positive correlation and PC1 shows negative correlation; Region 6 (1300-1152 cm^{-1}), where PC1 and PC3 show negative correlation and PC2 shows positive correlation except region 1260-1205 cm^{-1} in which PC1 shows positive correlation; Region 7 (1067-738 cm^{-1}), where PC1, PC2, and PC3 all show negative correlation; and Region 8 (750-665 cm^{-1}), where PC1 and PC2 show positive correlation and PC3 shows negative correlation. The results of loading plot in these spectra corresponding to the bloodstained fibers can be characterized by high intensity bands of amide I and amide II in the region 5 at 1640 cm^{-1} and 1540 cm^{-1} .

To validate the model, various non-blood substances were collected which could create ambiguity in investigators' mind to identify blood and non-blood substances due to their similar appearance. A total of 10 non-blood substances (3 each) including red lipstick, red eye-shadow, red nail polish, red ink, vermilion, honey, liquid hand wash, red blank fiber, red dye, and red skin toner were used. On the basis of visual analysis, spectrum obtained from each non-blood substance was easily discriminated from the spectrum of blood. However, visual analysis is a tedious process, and subjectivity in the interpretation of results could lead to false identification. PCA was applied to discriminate blood from these non- blood substances. As shown in Figure-5a, PCA score plot showed that the spectra of blood are widely dispersed along with PC3 axis. It is observed that the spectra of non- blood substances were distributed away from the spectrum of neat blood. In

this case PC1, PC2, and PC3 accounted for 52%, 21%, and 12% variations, respectively. In total, cumulative variance of 85% was obtained using PCA model. Figure-5b shows the combined loading plot of PC1, PC2, and PC3. The loading plot can be divided into 4 regions. Region 1 (3996- 3054 cm^{-1}), where PC1, PC2, and PC3 show positive correlation except in the range of 3448-3166 cm^{-1} , where PC3 shows positive as well as negative correlation. Region 2 (3040-1719 cm^{-1}), where PC1 and PC3 both show positive correlation and only PC2 shows a negative correlation. In region 3 (1699-1162 cm^{-1}) PC1 shows positive correlation and both PC2 and PC3 show negative correlation. In region 4 (1089-600 cm^{-1}) both PC2 and PC3 show positive correlation and PC1 shows a negative correlation.

On the basis of validation test, various parameters such as sensitivity, specificity, accuracy, false positive and false negative rate were calculated using the following formulas [53,79].

- Sensitivity = True positives/ True positives + False negatives $\times 100$
- Specificity = True negative/ True Negatives +False Positives $\times 100$
- Accuracy = True positive + True negative / (True positive + True negative + False positive + False negative) $\times 100$
- False positive rate= (False positive / (True positive + False negative) $\times 100$
- False negative rate = (False negative / (True negativ e+ false positive) $\times 100$

A PCA model was generated in response to two outputs: "blood" or "non-blood substances". The model achieved 100% accuracy, sensitivity, and specificity with 0% rate of false positives and negative classification.

4. Conclusions

The results of the present study suggest that ATR FT-IR spectroscopy can be successfully applied for forensic detection of blood stains on fibers of different types and colors, even when single fiber has been recovered. The results of present study are inherently significant in establishing ATR FT-IR spectroscopy as a rapid, reliable, cost effective, and a non-destructive alternative to other conventional methods. Moreover, it must be noted that it can conclusively and significantly differentiate blood samples on single fibers of different colors and types. Another facet to its advantage comes from the role of chemometric tools in interpretation of ATR FT-IR results. Chemometric tools such as PCA must be credited



to extract interpretable information from large pool of data obtained in the form of ATR FT-IR spectra. Using visual examination all blank fibers and bloodstained fibers could easily be discriminated on the basis of characteristic peaks positioned at approximately 1650 cm^{-1} and 1543 cm^{-1} corresponding to amide I and amide II, however, blank human hair fibers were overlapped with bloodstained fibers in the same region. Furthermore, PCA was applied to support the results of visual analysis which also classified the blank fiber spectra and spectra of bloodstained fibers objectively in separate clusters with 98% of variance in the range of 1700-1500 cm^{-1} , except bloodstained human hair samples. Since this is a preliminary study, it must be augmented with further studies using a higher number of samples and other chemometric tools for the detection of blood in simulated forensic casework conditions as well as discrimination and classification from other body fluids such as semen, saliva, etc. The use of ATR FT-IR spectroscopy is envisioned for the rapid, reliable and non-destructive detection of blood traces at the crime scene in an eco-friendly way.

Acknowledgements

The authors sincerely thank University Grants Commission (UGC), Ministry of Human Resource Development, Govt. of India for financial assistance for providing laboratory facilities in the Department of Forensic Science, Punjabi University Patiala. We would also like to extend our humble gratitude and vote of thanks to Bhanu Prakash R (Scientific advisor), SCIENCE4U Analytics and Research Solutions Pvt. Ltd., Bangalore, India, who has helped us in application of chemometric tools and interpretation of results and without whose help this study would not have reached its intended results.

Conflict of interest

No personal and financial relationships with any individual or organization that can raise conflict of interest with the present study.

Funding

None to declare

References

1. Virkler K, Lednev IK. Analysis of body fluids for forensic purposes: From laboratory testing to non-destructive rapid confirmatory identification at a crime scene. *Forensic Sci Int.* 2009;188:1–17. doi:10.1016/j.forsciint.2009.02.013.
2. Orphanou CM. The detection and discrimination of human body fluids using ATR FT-IR spectroscopy. *Forensic Sci Int.* 2015;252:e10–6. doi:10.1016/j.forsciint.2015.04.020.
3. An JH, Shin KJ, Yang WI, Lee HY. Body fluid identification in forensics, *BMB Rep.* 2012; 45: 545–553. doi:10.5483/bmbrep.2012.45.10.206.
4. Zapata F, Fernández de la Ossa MÁ, García-Ruiz C. Emerging spectrometric techniques for the forensic analysis of body fluids. *TrAC - Trends Anal Chem* 2015;64:53–63. doi:10.1016/j.trac.2014.08.011.
5. Zapata F, Silva Gregório Martins M. Body Fluids and Spectroscopic Techniques in Forensics: A Perfect Match? *Journal of forensic medicine.* 2016; 1: 1-7. doi:10.4172/2472-1026.1000101.
6. Bai P, Deng W, Wang L, Long B, Liu K, Liang W, et al. Micro RNA profiling for the detection and differentiation of body fluids in forensic stain analysis. *Forensic Sci Int Genet Suppl Ser.* 2013;4:e216–7. doi:10.1016/j.fsigss.2013.10.111.
7. Li Z, Bai P, Peng D, Long B, Zhang L, Liang W. Influences of different RT-qPCR methods on forensic body fluid identification by microRNA. *Forensic Sci Int Genet Suppl Ser.* 2015;5:295–7. doi:10.1016/j.fsigss.2015.09.117.
8. Courts C, Madea B. Specific Micro-RNA Signatures for the Detection of Saliva and Blood in Forensic Body-fluid Identification. *J Forensic Sci.* 2011;56:1464–70. doi:10.1111/j.1556-4029.2011.01894.x.
9. Hanson EK, Mirza M, Reka K, Ballantyne J. The identification of menstrual blood in forensic samples by logistic regression modeling of miRNA expression. *Electrophoresis* 2014;35:3087–95. doi:10.1002/elps.201400171.
10. Hanson E, Lubenow H, Ballantyne J. Identification of forensically relevant body fluids using a panel of differentially expressed microRNAs. *Forensic Sci Int Genet Suppl Ser.* 2009;2:503–4. doi:10.1016/j.fsigss.2009.08.184.
11. Zubakov D, Boersma AWM, Choi Y, Kayser M. MicroRNA markers for forensic body fluid identification obtained from microarray screening and quantitative RT-PCR confirmation. *Int J Legal Med.* 2010;217–26. doi:10.1007/s00414-009-0402-3.
12. Haas C, Klessner B, Maake C, Bär W, Kratzer A. mRNA profiling for body fluid identification by reverse transcription endpoint PCR and realtime PCR. *Forensic Sci Int Genet.* 2009;3:80–8. doi:10.1016/j.fsiggen.2008.11.003.
13. Juusola J, Ballantyne J. Multiplex mRNA profiling for the identification of body fluids. *Forensic Sci Int.*



- 2005;152:1–12. doi:10.1016/j.forsciint.2005.02.020.
14. Fleming R, Harbison S, Lin M. New RNA methods for the identification of body fluids and cell types. *Forensic Sci Int Genet Suppl Ser.* 2013;4:e87–8. doi:10.1016/j.fsigss.2013.10.044.
 15. Wang S, Wang Z, Tao R, He G, Liu J, Li C. The potential use of Piwi-interacting RNA biomarkers in forensic body fluid identification: A proof-of-principle study. *Forensic Sci Int Genet.* 2019;39:129–35. doi:10.1016/j.fsigen.2019.01.002.
 16. Liu B, Song F, Yang Q, Zhou Y, Shao C, Shen Y, et al. Characterization of tissue-specific biomarkers with the expression of circRNAs in forensically relevant body fluids. *Int J Legal Med.* 2019;1–11. doi: 10.1007/s00414-019-02027-y
 17. An JH, Choi A, Shin K. DNA methylation-specific multiplex assays for body fluid identification. *Int J Leg Med.* 2013;127:35–43. doi:10.1007/s00414-012-0719-1.
 18. Antunes J, Silva DSBS, Balamurugan K, Duncan G, Alho CS, Mccord B. High-resolution melt analysis of DNA methylation to discriminate semen in biological stains. *Anal Biochem.* 2016;494:40–5. doi:10.1016/j.ab.2015.10.002.
 19. Choi A, Shin KJ, Yang WI, Lee HY. Body fluid identification by integrated analysis of DNA methylation and body fluid-specific microbial DNA. *Int J Legal Med.* 2014;128:33–41. doi:10.1007/s00414-013-0918-4.
 20. Gomaa R, Salehi J, Behl S. DNA Methylation as a Biomarker for Body Fluid Identification. *Arab J Forensic Sci Forensic Med.* 2017;1:681–94. doi:10.26735/16586794.2017.001.
 21. Facht C, Quarino L. High resolution melt curve analysis based on methylation status for human semen identification. *Forensic Sci Med Pathol.* 2017;86–91. doi:10.1007/s12024-016-9825-6.
 22. Forat S, Huettel B, Reinhardt R, Fimmers R, Haidl G, Denschlag D, et al. Methylation Markers for the Identification of Body Fluids and Tissues from Forensic Trace Evidence. *PLoS ONE.* 2016;1–19. doi:10.1371/journal.pone.0147973.
 23. Frumkin D, Wasserstrom A, Budowle B, Davidson A. DNA methylation-based forensic tissue identification. *Forensic Sci Int Genet.* 2011;5:517–24. doi:10.1016/j.fsigen.2010.12.001.
 24. Fu XD, Wu J, Wang J, Huang Y, Hou YP, Yan J. Identification of body fluid using tissue-specific DNA methylation markers. *Forensic Sci Int Genet Suppl Ser.* 2015;5:151–3. doi: 10.1016/j.fsigen.2014.07.011.
 25. Gomes I, Kohlmeier F, Schneider PM. Genetic markers for body fluid and tissue identification in forensics. *Forensic Sci Int Genet Suppl Ser.* 2011;3:e469–70. doi:10.1016/j.fsigss.2011.09.096.
 26. Zrnc D, Vickovic S, Grs B, Popovic M. DNA methylation: the future of crime scene investigation? *Mol Biol Rep.* 2013;4349–60. doi:10.1007/s11033-013-2525-3.
 27. Auvdel MJ. Comparison of laser and ultraviolet techniques used in the detection of body secretions. *J Forensic Sci.* 1987;32:326–45. doi: 10.1520/JFS11136J.
 28. Vandenberg N, van Oorschot RAH. The Use of Polilight® in the Detection of Seminal Fluid, Saliva, and Bloodstains and Comparison with Conventional Chemical-Based Screening Tests. *J Forensic Sci.* 2006;51:361–70. doi:10.1111/j.1556-4029.2006.00065.x.
 29. Fiedler A, Rehdorf J, Hilbers F, Johrdan L, Stribl C, Benecke M. Detection of Semen (Human and Boar) and Saliva on Fabrics by a Very High Powered UV/VIS-Light Source. *Open Forensic Sci J.* 2008;1:12–5. doi:10.2174/1874402800801010012
 30. Zapata F, de la Ossa MÁF, García-Ruiz C. Differentiation of Body Fluid Stains on Fabrics Using External Reflection Fourier Transform Infrared Spectroscopy (FT-IR) and Chemometrics. *Appl Spectrosc.* 2016;70:654–65. doi:10.1177/0003702816631303.
 31. Muro CK, Doty KC, Bueno J, Halámková L, Lednev IK. Vibrational Spectroscopy: Recent Developments to Revolutionize Forensic Science. *Anal Chem.* 2015;87:306–27. doi:10.1021/ac504068a.
 32. Boyd S, Bertino MF, Ye D, White LS, Seashols SJ. Highly Sensitive Detection of Blood by Surface Enhanced Raman Scattering. *J Forensic Sci.* 2013;58:753–6. doi:10.1111/1556-4029.12120.
 33. Muro CK, Doty KC, de Souza Fernandes L, Lednev IK. Forensic body fluid identification and differentiation by Raman spectroscopy. *Forensic Chem.* 2016;1:31–8. doi:10.1016/j.forc.2016.06.003.
 34. Virkler K, Lednev IK. Raman spectroscopic signature of semen and its potential application to forensic body fluid identification. *Forensic Sci Int.* 2009;193:56–62. doi:10.1016/j.forsciint.2009.09.005.
 35. Sikirzhytski V, Sikirzhytskaya A, Lednev IK. Multidimensional Raman spectroscopic signature of sweat and its potential application to forensic body fluid identification. *Anal Chim Acta.* 2012;718:78–83. doi:10.1016/j.aca.2011.12.059.
 36. Feine I, Gafny R, Pinkas I. Combination of prostate-specific antigen detection and micro-Raman spectroscopy for confirmatory semen detection.



- Forensic Sci Int. 2017;270:241–7. doi:10.1016/j.forsciint.2016.10.012.
37. Huang Z, Chen X, Chen Y, Feng S, Chen R, Chen J, et al. Raman spectroscopic characterization and differentiation of seminal plasma. *J Biomed Opt.* 2011;16:1–4. doi:10.1117/1.3650310
38. McLaughlin G, Sikirzhytski V, Lednev IK. Circumventing substrate interference in the Raman spectroscopic identification of blood stains. *Forensic Sci Int.* 2013;231:157–66. doi:10.1016/j.forsciint.2013.04.033.
39. McLaughlin G, Lednev IK. In Situ Identification of Semen Stains on Common Substrates via Raman Spectroscopy. *J Forensic Sci.* 2015;60:595–604. doi:10.1111/1556-4029.12708.
40. McLaughlin G, Doty KC, Lednev IK. Raman Spectroscopy of Blood for Species Identification. *Anal Chem.* 2014;86:11628–33. doi:10.1021/ac5026368.
41. Doty KC, Lednev IK. Differentiation of human blood from animal blood using Raman spectroscopy: A survey of forensically relevant species. *Forensic Sci Int.* 2018;282:204–10. doi:10.1016/j.forsciint.2017.11.033.
42. Fujihara J, Fujita Y, Yamamoto T, Nishimoto N, Kimura-Kataoka K, Kurata S, et al. Blood identification and discrimination between human and nonhuman blood using portable Raman spectroscopy. *Int J Legal Med.* 2017;131:319–22. doi:10.1007/s00414-016-1396-2.
43. Virkler K, Lednev IK. Blood Species Identification for Forensic Purposes Using Raman Spectroscopy Combined with Advanced Statistical Analysis. *Anal Chem.* 2009;81:7773–7. doi:10.1021/ac901350a.
44. Mistek E, Halámková L, Doty KC, Muro CK, Lednev IK. Race Differentiation by Raman Spectroscopy of a Bloodstain for Forensic Purposes. *Anal Chem.* 2016;88:7453–6. doi:10.1021/acs.analchem.6b01173.
45. Muro CK, Lednev IK. Race Differentiation Based on Raman Spectroscopy of Semen Traces for Forensic Purposes. *Anal Chem.* 2017;89:4344–8. doi:10.1021/acs.analchem.7b00106.
46. Muro CK, de Souza Fernandes L, Lednev IK. Sex Determination Based on Raman Spectroscopy of Saliva Traces for Forensic Purposes. *Anal Chem.* 2016;88:12489–93. doi:10.1021/acs.analchem.6b03988.
47. Sikirzhytskaya A, Sikirzhytski V, K Lednev I. Raman spectroscopy coupled with advanced statistics for differentiating menstrual and peripheral blood. *Journal of biophotonics.* 2014; 7: 59-67 doi:10.1002/jbio.201200191.
48. Zapata F, Fernández de la Ossa MÁ, García-Ruiz C. Emerging spectrometric techniques for the forensic analysis of body fluids. *TrAC Trends Anal Chem* 2015;64:53–63. doi:10.1016/j.trac.2014.08.011.
49. Quinn AA, Elkins KM. The Differentiation of Menstrual from Venous Blood and Other Body Fluids on Various Substrates Using ATR FT-IR Spectroscopy. *J Forensic Sci* 2017;62:197–204. doi:10.1111/1556-4029.13250.
50. Gregório I, Zapata F, García-Ruiz C. Analysis of human bodily fluids on superabsorbent pads by ATR-FTIR. *Talanta* 2017;162:634–40. doi:10.1016/j.talanta.2016.10.061.
51. Elkins KM. Rapid Presumptive “Fingerprinting” of Body Fluids and Materials by ATR FT-IR Spectroscopy. *J Forensic Sci.* 2011;56:1580–7. doi:10.1111/j.1556-4029.2011.01870.x.
52. De Wael K, Lepot L, Gason F, Gilbert B. In search of blood—Detection of minute particles using spectroscopic methods. *Forensic Sci Int.* 2008;180:37–42. doi:10.1016/j.forsciint.2008.06.013.
53. Gregório I, Zapata F, Torre M, García-Ruiz C. Statistical approach for ATR-FTIR screening of semen in sexual evidence. *Talanta* 2017;174:853–7. doi:10.1016/j.talanta.2017.07.016.
54. Sharma S, Chopra R, Singh R. Forensic discrimination of menstrual blood and peripheral blood using attenuated total reflectance (ATR)-Fourier transform infrared (FT-IR) spectroscopy and chemometrics. *Int J Legal Med* 2019. doi:10.1007/s00414-019-02134-w.
55. Lin H, Zhang Y, Wang Q, Li B, Huang P, Wang Z. Estimation of the age of human bloodstains under the simulated indoor and outdoor crime scene conditions by ATR-FTIR spectroscopy. *Sci Rep.* 2017;7:13254. doi:10.1038/s41598-017-13725-1.
56. Lin H, Zhang Y, Wang Q, Li B, Fan S, Wang Z. Species identification of bloodstains by ATR-FTIR spectroscopy: the effects of bloodstain age and the deposition environment. *Int J Legal Med.* 2018;132:667–74. doi:10.1007/s00414-017-1634-2.
57. Zhang Y, Wang Q, Li B, Wang Z, Li C, Yao Y, et al. Changes in Attenuated Total Reflection Fourier Transform Infrared Spectra as Blood Dries Out. *J Forensic Sci.* 2017; 62:761–7. doi:10.1111/1556-4029.13324.
58. Takamura A, Watanabe K, Akutsu T, Ozawa T. Soft and Robust Identification of Body Fluid Using Fourier Transform Infrared Spectroscopy and Chemometric Strategies for Forensic Analysis. *Sci Rep.* 2018;8:8459. doi:10.1038/s41598-018-26873-



- 9.
59. Takamura A, Watanabe K, Akutsu T, Ikegaya H, Ozawa T. Spectral Mining for Discriminating Blood Origins in the Presence of Substrate Interference via Attenuated Total Reflection Fourier Transform Infrared Spectroscopy: Postmortem or Antemortem Blood? *Anal Chem*. 2017;89:9797–804. doi:10.1021/acs.analchem.7b01756.
60. Takamura A, Halamkova L, Ozawa T, Lednev IK. Phenotype Profiling for Forensic Purposes: Determining Donor Sex Based on Fourier Transform Infrared Spectroscopy of Urine Traces. *Anal Chem*. 2019;91:6288–95. doi:10.1021/acs.analchem.9b01058.
61. Zhang K, Wang Q, Liu R, Wei X, Li Z, Fan S, et al. Evaluating the effects of causes of death on postmortem interval estimation by ATR-FTIR spectroscopy. *Int J Legal Med*. 2019. doi:10.1007/s00414-019-02042-z.
62. Lu Z, DeJong SA, Cassidy BM, Belliveau RG, Myrick ML, Morgan SL. Detection Limits for Blood on Fabrics Using Attenuated Total Reflection Fourier Transform Infrared (ATR FT-IR) Spectroscopy and Derivative Processing. *Appl Spectrosc*. 2016;71:839–46. doi:10.1177/0003702816654154.
63. Cai S, Singh BR. Identification of β -turn and random coil amide III infrared bands for secondary structure estimation of proteins. *Biophys Chem* 1999;80:7–20. doi:10.1016/S0301-4622(99)00060-5.
64. Garside P, Wyeth P. Identification of Cellulosic Fibres by FTIR Spectroscopy I: Thread and Single Fibre Analysis by Attenuated Total Reflectance. *Studies in Conservation*. 2003; 48:269-275. doi:10.2307/1506916.
65. Peets P, Leito I, Pelt J, Vahur S. Identification and classification of textile fibres using ATR-FT-IR spectroscopy with chemometric methods. *Spectrochim Acta Part A Mol Biomol Spectrosc*. 2017;173:175–81. doi:10.1016/j.saa.2016.09.007.
66. Lang PL, Katon JE, O'Keefe JF, Schiering DW. The identification of fibers by infrared and Raman microspectroscopy. *Microchem J*. 1986;34:319–31. doi:10.1016/0026-265X(86)90127-X.
67. Chen H, Lin Z, Tan C. Classification of different animal fibers by near infrared spectroscopy and chemometric models. *Microchem J*. 2019;144:489–94. doi:10.1016/j.microc.2018.10.011.
68. Kumar R, Sharma V. Chemometrics in forensic science. *TrAC Trends Anal Chem* 2018;105:191–201. doi:10.1016/j.trac.2018.05.010.
69. Silva CS, Pimentel MF, Amigo JM, Honorato RS, Pasquini C. Detecting semen stains on fabrics using near infrared hyperspectral images and multivariate models. *TrAC Trends Anal Chem*. 2017;95:23–35. doi:10.1016/j.trac.2017.07.026.
70. Gautam R, Vanga S, Ariese F, Umapathy S. Review of multidimensional data processing approaches for Raman and infrared spectroscopy. *EPJ Tech Instrum*. 2015;2:8. doi:10.1140/epjti/s40485-015-0018-6.
71. Lee LC, Liong C-Y, Jemain AA. A contemporary review on Data Preprocessing (DP) practice strategy in ATR-FTIR spectrum. *Chemom Intell Lab Syst* 2017;163:64–75. doi:10.1016/j.chemolab.2017.02.008.
72. Narayanan K, Thirunavukkarasu M, Esther Jeyanthi C, Shenbagarajan P. FTIR and UV-visible spectral study on normal blood samples. *Int J Pharma. Bio. Sci*. 2011; 1:74-81.
73. Chung C, Lee M, Choe EK. Characterization of cotton fabric scouring by FT-IR ATR spectroscopy. *Carbohydr Polym* 2004;58:417–20. doi:10.1016/j.carbpol.2004.08.005.
74. Li L, Frey M, Browning KJ. Biodegradability Study on Cotton and Polyester Fabrics. *J Eng Fiber Fabr*. 2010; 42-53. doi:10.1177/155892501000500406.
75. Kong J, Yu S. Fourier Transform Infrared Spectroscopic Analysis of Protein Secondary Structures. *Acta Biochim Biophys Sin (Shanghai)* 2007;39:549–59. doi:10.1111/j.1745-7270.2007.00320.x.
76. Dong A, Huang P, Caughey WS. Protein secondary structures in water from second-derivative amide I infrared spectra. *Biochemistry* 1990;29:3303–8. doi:10.1021/bi00465a022.
77. Pelton JT, McLean LR. Spectroscopic Methods for Analysis of Protein Secondary Structure. *Anal Biochem*. 2000; 277:167–76. doi:10.1006/abio.1999.4320.
78. Haris PI. Probing protein–protein interaction in biomembranes using Fourier transform infrared spectroscopy. *Biochim Biophys Acta - Biomembr*. 2013;1828:2265–71. doi:10.1016/j.bbamem.2013.04.008.
79. Morillas AV, Gooch J, Frascione N. Feasibility of a handheld near infrared device for the qualitative analysis of bloodstains. *Talanta*. 2018;184:1–6. doi:10.1016/j.talanta.2018.02.110.

